

Supplementary Information

SMART FRAP: a robust and quantitative FRAP analysis method for phase separation

Xiaotian Wang^{ab}, Jiahao Niu^{ab}, Yi Yang^a, Yao Wang^{ab} and Yujie Sun^{*ab}

a. School of Life Sciences, State Key Laboratory of Membrane Biology, Biomedical Pioneering Innovation Center (BIOPIC), Peking University, Beijing, China.

b. National Biomedical Imaging Center, College of Future Technology, Peking University, Beijing, China.

*. Corresponding authors.

Table of Contents

Methods.....	2
Expression and purification of FUS and its mutant	2
In vitro phase separation experiment	2
Confocal microscopy	2
FRAP experiment	2
Single molecule tracking	3
Euclidean distance	3
Details of modelling	3
Fitting formulas for FRAP analysis	4
Statistics and reproducibility	5
Code availability	5
Supplementary Figures	6

Methods

Expression and purification of FUS and its mutant

The bacterial protein expression vector is pet28. FUS and G156E mutants were recombined with MBP-tag on the N-terminal, mCherry-tag or mMaple3-tag on the C-terminal, and 6*HIS-tag on the N-terminal of MBP-tag. The plasmid was transformed into BL21 (DE3) *E. coli*. Culture overnight on LB agar plate. The monoclonal was inoculated with 0.5 L LB and cultured to OD₆₀₀ of approximately 0.8 at 37°C. Bacteria were harvested after overnight induction with 1 mM IPTG at 18°C. The cells were collected by centrifugation at 5200 g for 15 min and the precipitates were re-suspended in lysis buffer (50 mM Tris-HCl (pH 7.4), 1 M KCl, 10 mM Imidazole, 1.5 mM βME, and 5 % Glycerol) and sonicated on ice. All purification steps were performed at 4°C to maintain protein activity. The lysates were centrifuged at 25000 g for 40 min and the supernatant was collected. A nickel-nitrilotriacetic acid (Ni-NTA) affinity column resin was used to bind the HIS-tagged recombinant protein, and the beads were washed with wash buffer (50 mM Tris-HCl (pH 7.4), 1 M KCl, 50 mM Imidazole, 1.5 mM βME, and 5 % Glycerol). Finally, the protein was eluted with elute buffer (50 mM Tris-HCl (pH 7.4), 1 M KCl, 500 mM Imidazole, 1.5 mM βME, and 5% Glycerol). The protein was dialyzed into the phase separation buffer (50 mM Tris-HCl (pH 7.4), 150 mM KCl, 10 mM Imidazole, 1.5 mM βME, and 5 % Glycerol), concentrate to 20 μM and stored at -80°C.

In vitro phase separation experiment

The following methods are used for all proteins phase separation experiment in this paper. Melting and centrifuging the purified 20 μM protein solution, supernatant was taken to remove possible polymers and precipitates. The supernatant was mixed with phase separation buffer containing 20% PEG-8000 (50 mM Tris-HCl (pH 7.4), 150 mM KCl, 10mM Imidazole, 1.5 mM βME, 5% Glycerol and 20% PEG-8000) in a ratio of 1 to 1 to obtain 10 μM protein solution with 10% PEG-8000 in which phase separation could occur.

Confocal microscopy

Confocal microscopy imaging was performed using a Nikon TiE CSU-W1 spinning disk confocal, equipped with a 561 nm excitation laser and a sCMOS Prime 95B camera. The real-time SR structure lighting super resolution module is also used. Images were obtained using a 100× oil-immersed lens with NA 1.4. The sample was loaded to a homemade fluted slide for imaging.

FRAP experiment

Experiments were carried out on the confocal microscope introduced above. Full field of view has a pixel resolution of 65 nm × 65 nm and size of 1200 pixel × 1200 pixel. The mCherry-tagged protein condensates were bleached 5 times by a 561 nm laser at 10% power with a thickness of 10 μm. Two frames are taken before the bleaching begins with time interval of 5 s. One frame was taken immediately after the bleaching, followed by a series of photographs spaced 5 s apart. In order to reduce the effect of condensates interaction with the glass surface, the last layer of condensates is avoided during image acquisition.¹ We corrected natural photobleaching in the bleached region using the intensity in the unbleached region far away from the bleached region. In all FRAP

experiments, the photobleaching time point was defined as 0 s. The experiment was conducted at room temperature.

Single molecule tracking

Single-molecule images were taken on a custom Olympus IX83 inverted microscope with an oil-immersed objective of 100 \times , NA = 1.49 and an Andor iXon Ultra EMCCD. The laser power is modulated by an acousto-optic tunable filter (AOTF). We used total internal reflection fluorescence (TIRF) in all single molecule tracking experiments and carefully optimized the angle of the inclined light to reduce the background signal in the tracking experiments. For sparse tracking, the protein solution was pre-activated with a low-power 488 nm laser to transform mMaple3 from green to red state. We use time-lapse illumination with a camera exposure time of 10 ms. The video was recorded successively for 1 min with an interval of 50 ms.

All single molecule tracking data were analyzed using ImageJ plug-in Trackmate to obtain the trajectory.² Briefly, we detect a single molecule of protein using the Laplacian of Gaussian (LoG) detector with an estimated object diameter of 0.5 μm (160 nm per pixel, same as below) and a threshold of 100, combined with median filtering and sub-pixel localization. A simple linear assignment problem (LAP) tracker is used in the linking process, and set the parameters as: linking max distance, 0.5 μm ; gap-closing max distance, 0.5 μm ; gap-closing max frame gap, 2.

Mean square displacement analysis was performed using a customized MATLAB script. The 2D time-lag mean squared displacement (TMSD) of each track was calculated by

$$TMSD(n\Delta t) = (\vec{r}_{i+n} - \vec{r}_i)^2$$

where Δt is the time interval between frames, \vec{r}_i is the position of the molecule at i -th frame in its trajectory, \bar{x} is the mean value of x . The TMSD was fit to

$$TMSD(n\Delta t) = 4D(n\Delta t)^\alpha$$

to calculate the diffusion coefficient (D) and anomalous diffusion exponent (α). In order to make the calculation results more accurate and reasonable, only the values of n from 0 to 5 in TMSD are used in the fitting.

Euclidean distance

By resampling and normalizing the curve, the two fitting curves that need to be compared have the same sampling frequency. In this case, the Euclidean distance can be approximated as the area of the graph enclosed by the two curves. The smaller the value, the closer the two curves are.

$$Euclidean\ distance = \sum_i |y_{1i} - y_{2i}| \cdot \Delta x_i$$

Where y_{ni} is the intensity of normalized recovery curve at i -th point of sampling, Δx_i is the time interval between i -th and $(i+1)$ -th point.

Details of modelling

The flow chart is shown as Fig. S10.

Input of SMART FRAP:

stack images of FRAP condensate (.tif) and control condensate (.tif). Users should crop them from the raw FRAP image manually.

Output of SMART FRAP:

the standard format of Matlab data storage (.mat) containing the diffusion coefficient, mobile fraction, reactivity of the boundary, the parameters of the intermediate process and so on.

Details of SMART FRAP: part 1-Image processing:

Firstly, for the control images. For each frame, the foreground (condensate) and background are determined through the foreground recognition algorithm, and the edge of the condensate is determined and fitted by ellipse (Fig. S2a). The image drift in the process is determined by the position of fitted ellipse at different frames (Fig. S2c). The median of the background pixel values is subtracted from the image as a debackground processing to calculate the final fluorescence intensity of the control condensate to correct for natural photobleaching (Fig. S2d).

Then, for the bleached image. The frame of bleaching was determined by the fall of the total intensity of image, named as frame 0. The position of condensate at frame -1 was determined using a similar method as control condensates. The degree of bleaching in different positions of condensates was determined by comparing the intensity of condensates in frame -1 and frame 0, and the location of bleached region was fitted with a circle (Fig. S2a). The drift correction of bleaching condensates was made by using the drift of control condensates. After debackground and natural bleaching correction, the fluorescence recovery curve of the bleached region can then be determined.

Details of SMART FRAP: part 2-Initiation model and optimize parameters:

The size of the condensates, the bleaching position and bleach level was identified in the previous step. The three-dimensional ellipsoidal lattice condensates are reconstructed in proportions through these parameters. For particle swarm optimization (PSO) algorithm, its key parameters are: population size $m = 32$; inertia weight w starts at 0.9 and gradually decreases to 0.4; acceleration constant $c1 = 2$ and $c2 = 2$. For the same parameter combination, 8 independent calculations were carried out at the same time by using the built-in parallel operation in MATLAB, and the average of the recovery curve was taken as the final result. The simulated recovery curve was compared with the experimental curve, and the number of simulation steps was adjusted to obtain the simulation curve closest to the experimental curve within the current parameter combination. Iterate until a preset number of iteration steps or a preset error value is reached.

Fitting formulas for FRAP analysis

The common used FRAP fitting formula was compiled by Taylor et al. ³

Table S1 Expressions for the formulas with different boundary condition and dimensions

Type	Recovery curve
Simple exponential	$\langle C^* \rangle(t) = A \left(1 - \exp\left(-\frac{t}{\tau}\right) \right)$
1D fix boundary	$\langle C^* \rangle(t) = 1 - \sum_{n=0}^{\infty} \frac{8}{((2n+1)\pi)^2} \exp\left(-((2n+1)\pi)^2 t / (4\tau)\right)$
1D infinite boundary	$\langle C^* \rangle(t) = 1 - \operatorname{erf}\left(\left(\frac{t}{\tau}\right)^{1/2}\right) + \left(\frac{t}{\pi\tau}\right)^{1/2} \left[1 - \exp\left(-\frac{t}{\tau}\right) \right]$

2D fix boundary	$\langle C^* \rangle(t) = 1 - \sum_{n=0}^{\infty} \frac{4}{\alpha_n^2} \exp(-\alpha_n^2 t/\tau)$
2D infinite boundary	$\langle C^* \rangle(t) = \exp\left(-\frac{2\tau}{t}\right) \left[I_0\left(\frac{2\tau}{t}\right) + I_1\left(\frac{2\tau}{t}\right) \right]$
3D fix boundary	$\langle C^* \rangle(t) = 1 - \sum_{n=0}^{\infty} \frac{6}{(n\pi)^2} \exp(- (n\pi)^2 t/\tau)$
3D infinite boundary	$\langle C^* \rangle(t) = 1 - \operatorname{erf}\left(\left(\frac{\tau}{t}\right)^{1/2}\right) + \left(\frac{t}{\pi\tau}\right)^{1/2} \left[3 - \exp\left(-\frac{\tau}{t}\right) \right] + 2\left(\frac{t^3}{\pi\tau^3}\right)^{1/2} \left[\exp\left(-\frac{\tau}{t}\right) \right]$

Here $C(r,t)$ is the fluorescence intensity at distance r from time t . C^* is defined as $C^*(r,t) = (C(r,t) - C(r,0))/(C(R,t) - C(r,0))$ for the fix boundary condition and $C^*(r,t) = (C(r,t) - C(r,0))/(C(\infty,t) - C(r,0))$ for the infinity boundary condition, and $\langle C^* \rangle$ is defined as the averaged of C^* in the giving ROI. The error function is denoted by erf . α_n is the function zero of order zero modified Bessel function $J_0(\alpha_n) = 0$. $\tau = R^2/D$ for all formulas.

Statistics and reproducibility

All experiments were conducted independently at least three times. All statistical tests were two-sided, and a P value less than 0.05 was considered statistically significant. All the boxes in the boxplot extend from the 25th percentile to the 75th percentile; The line in the box represents the median, and the whiskers represent the range within the 1.5 times of interquartile range.

Code availability

Code for SMART FRAP has been deposited to Zenodo (10.5281/zenodo.7330165).

Supplementary Figures

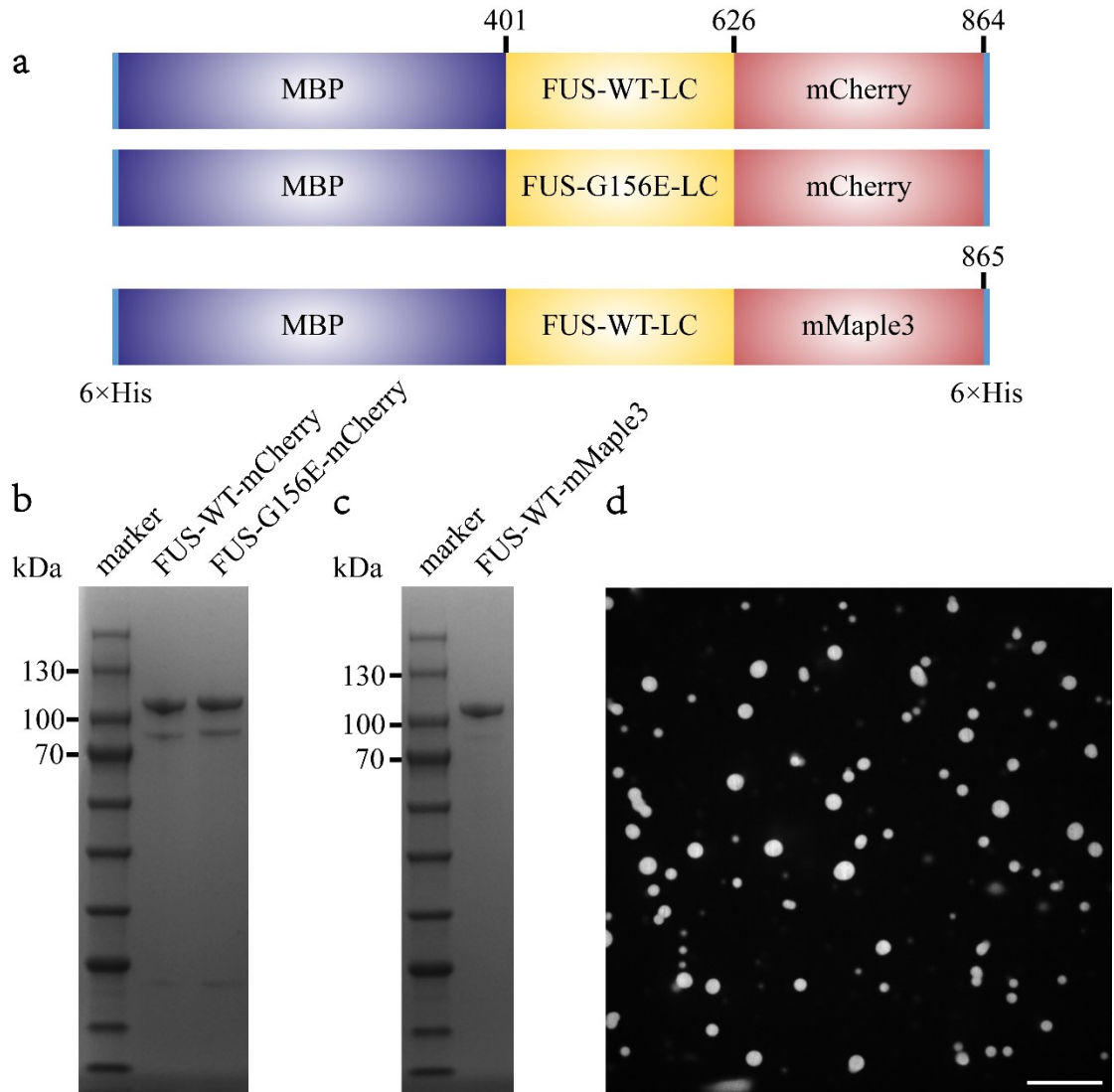


Figure S1. (a) Domain structure of recombinant FUS and mutant. (b-c) SDS PAGE of in vitro purified (b) FUS-WT-mCherry, FUS-G156E-mCherry, (c) FUS-WT-mMaple3. (d) Confocal image of 10 μ M FUS-mCherry phase separation with 10% PEG-8000. Scale bar, 20 μ m.

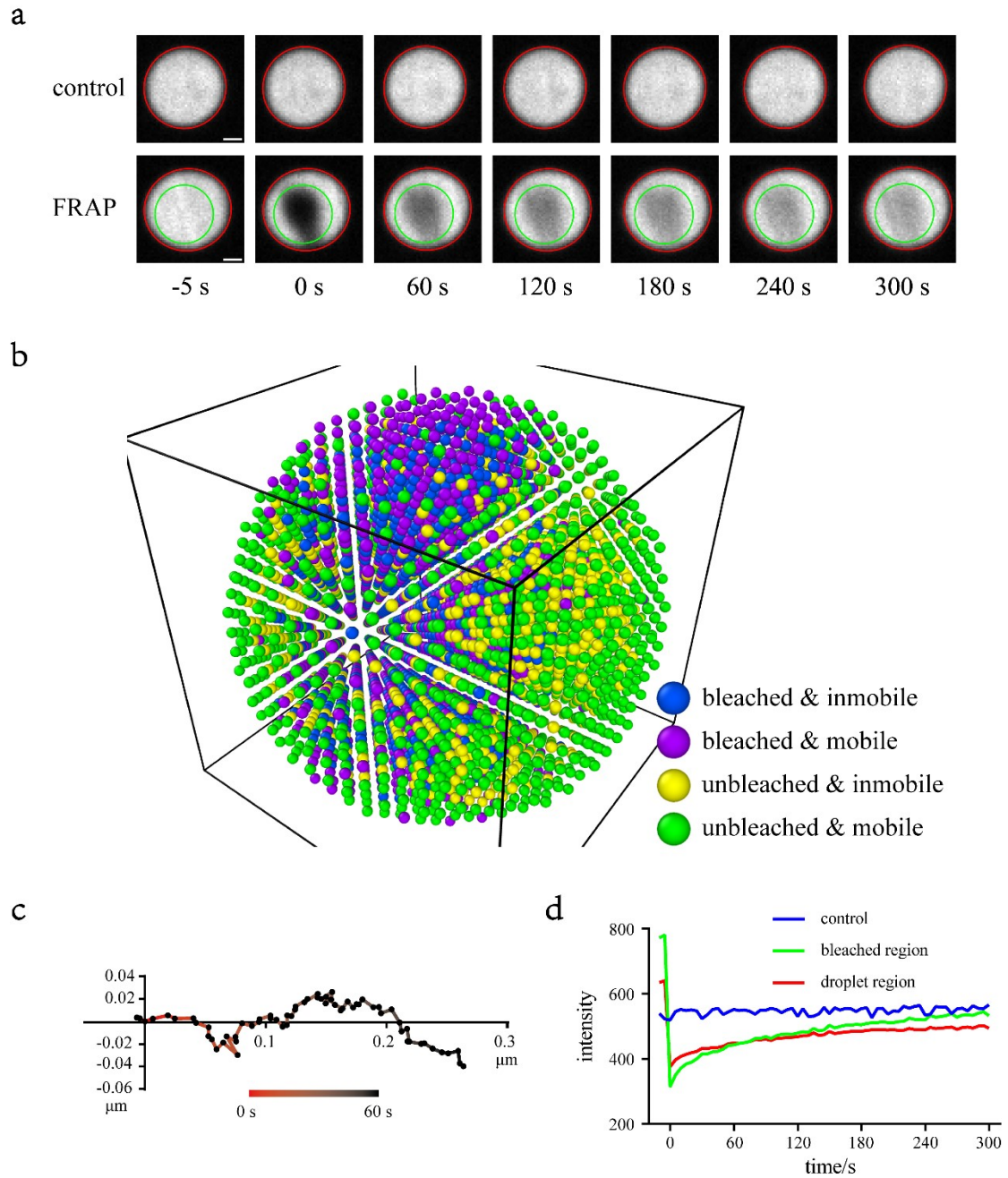


Figure S2. (a) Example fluorescence images of control condensate (upper) and FRAP condensate (lower) of FUS. Condensate region (red) and bleached region (green) that the program automatically identifies are labeled on the image. Scale bar, $1\mu\text{m}$. (b) the initial state of the lattice model constructed from (a), mobile fraction set as 0.5. (c) Drift of the condensate identified by the program. trajectory is color-coded according to its time from 0 s (red) to 300 s (black). (d) Fluorescence intensity curves corresponding to different regions. Blue, the control condensate region, red the FRAP condensate region and green, the bleached region.

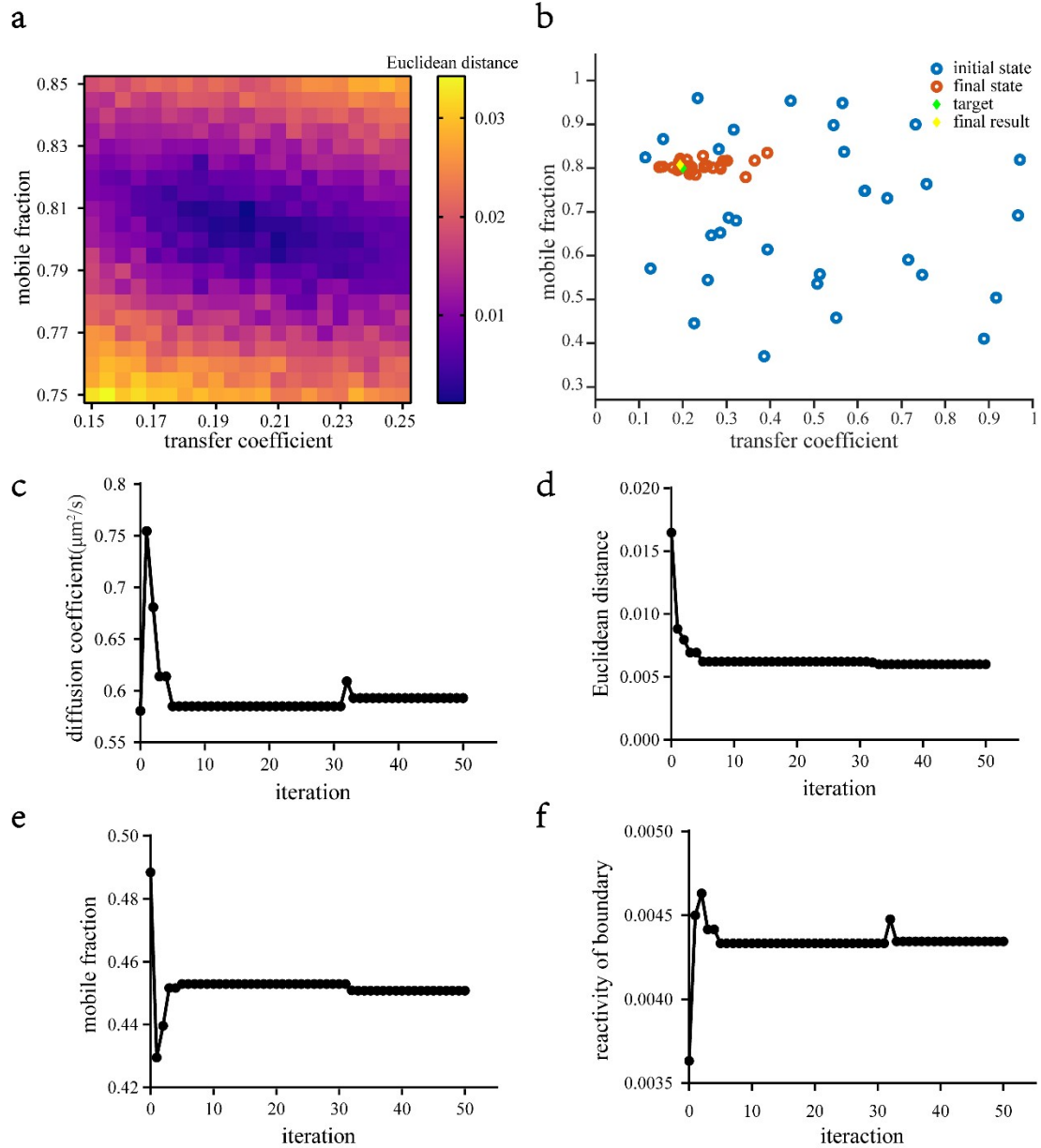


Figure S3. (a) An example of energy landscape of SMART FRAP. Loss function is defined as the Euclidean distance between recovery curve with (mobile fraction = 0.8, transfer coefficient = 0.2) and curves in parameter space ($0.75 < \text{mobile fraction} < 0.85$, $0.15 < \text{transfer coefficient} < 0.25$). (b) An example of PSO process of SMART FRAP. Blue circles indicate 32 initial states, red circles indicate 32 final states after 10 iterations, green diamond marks the optimization target, yellow diamond marks the final optimization result. (c-f) Parameters fluctuation during iteration. (c) Diffusion coefficient, (d) Euclidean distance, (e) mobile fraction and (f) reactivity of boundary.

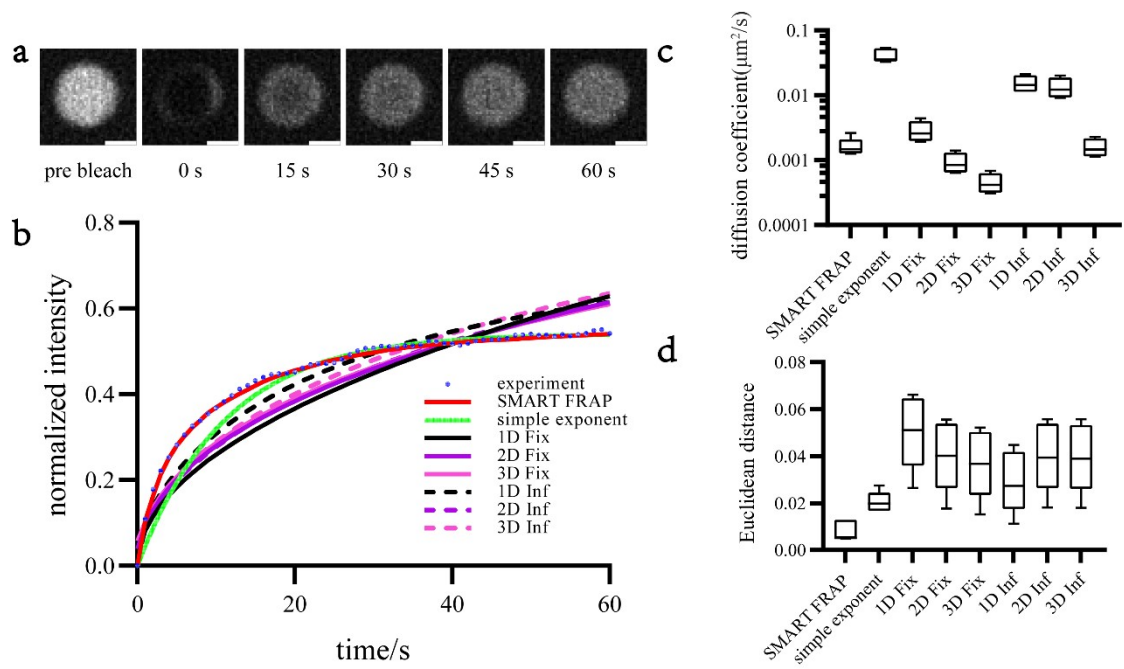


Figure S4. (a) Example fluorescence images of FRAP condensate of 22.5 μM full length PML with 4% PEG-8000. Scale bar, 1 μm (b) FRAP recovery curve of experiment, SMART FRAP, and fitting formulas of full length PML. (c) Boxplot of diffusion coefficient calculated by SMART FRAP and fitting formulas. Sample size: 5. (d) Boxplot of Euclidean distance between the experiment recovery curve and curves calculated by SMART FRAP or fitting formulas in (c).

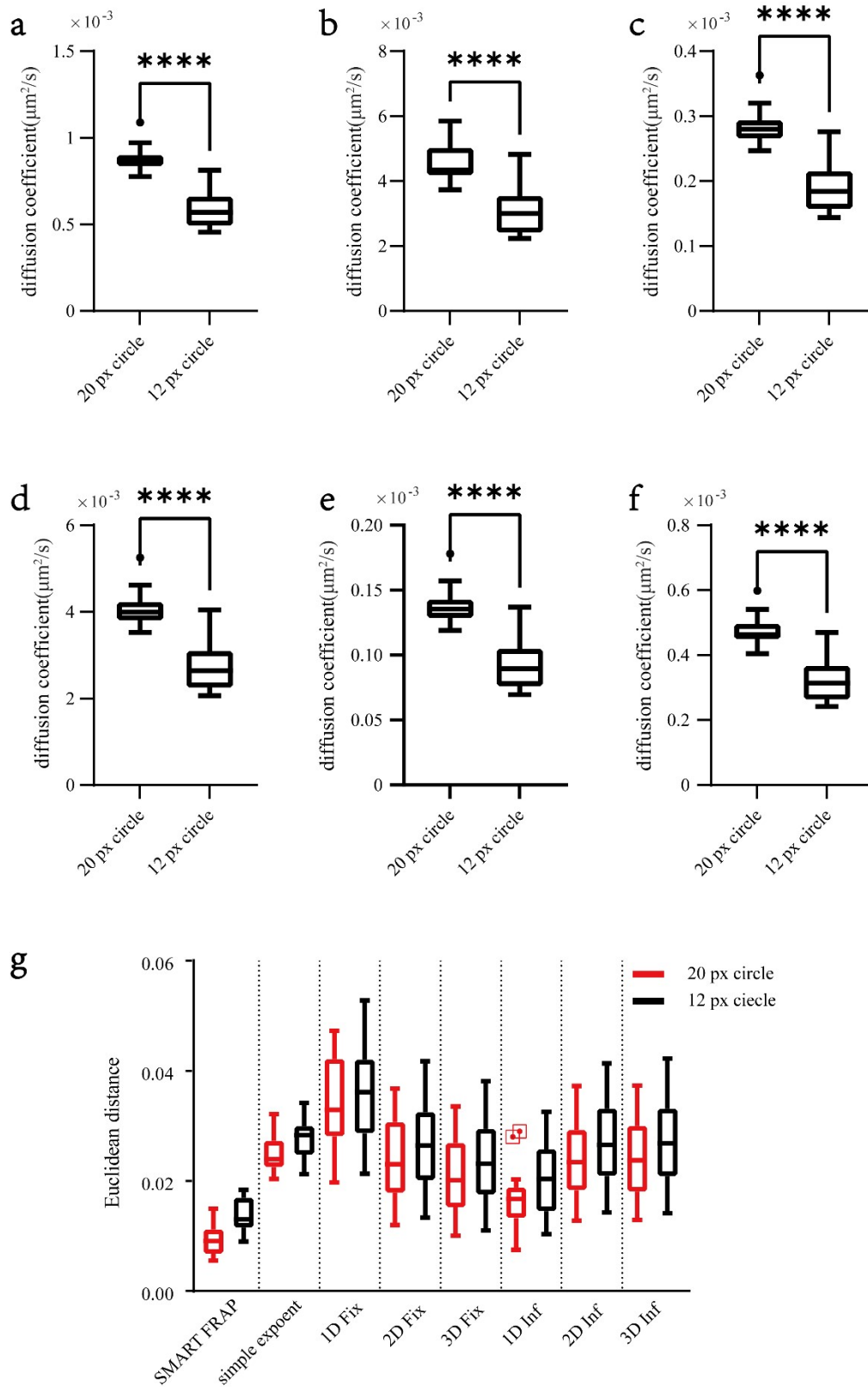


Figure S5. (a-f) Boxplot of diffusion coefficient with different bleached regions calculated by (a) 1D Fix, (b) 2D Fix, (c) 3D Fix, (d) 1D Inf, (e) 2D Inf, (f) 3D Inf. Fitting formulas in Table S1. (g) Boxplot of Euclidean distance between the experimental curve and curves calculated by SMART FRAP or fitting formulas with different bleached region size. Sample size: 14.

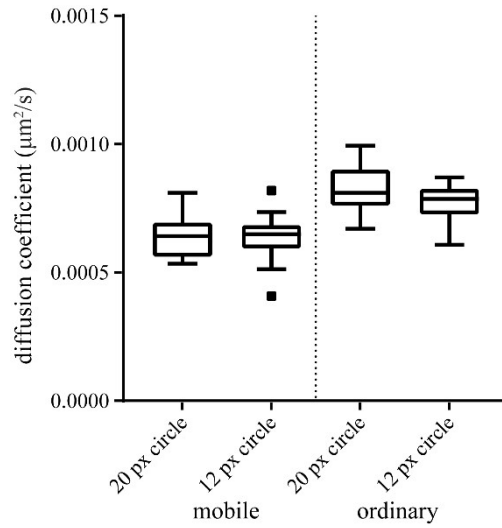


Figure S6. Diffusion coefficient for different bleached regions using ordinary and mobile boundaries. Sample size: 14.

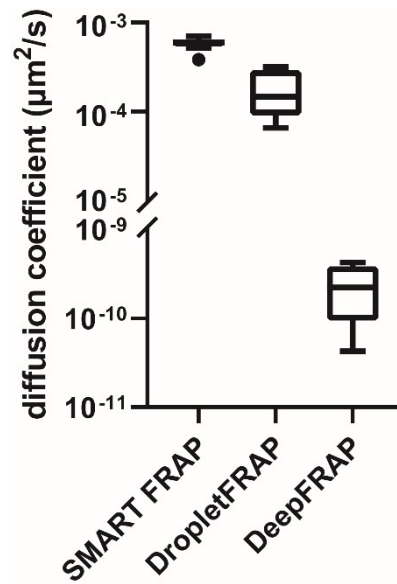


Figure S7. Comparison of diffusion coefficients calculated by SMART FRAP and previously published models, DropletFRAP and DeepFRAP.^{4, 5}

Parameters in DropletFRAP are set as pixel size: 0.065 μm, frame interval: 5 s, number of frames to be analyzed: 60, starting frame: 2, PDE model: 'simple_drop', edge correction: 0, camera background: 150, geometry: 1, respectively. Default parameters and models are used in DeepFRAP.

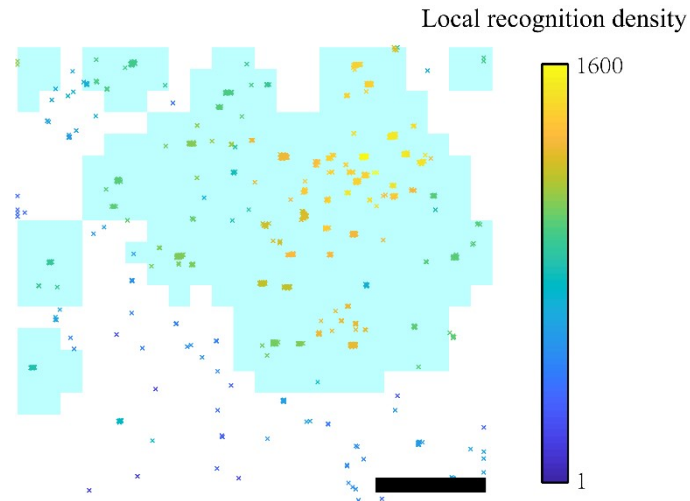


Figure S8. Localizations recognized during the stacks of 1200 frames imaging of FUS-mMaple3. Local recognition density is defined as the number of detected spots within a local circle with the radius of 2 pixels at this position. Scale bar, 5 μm .

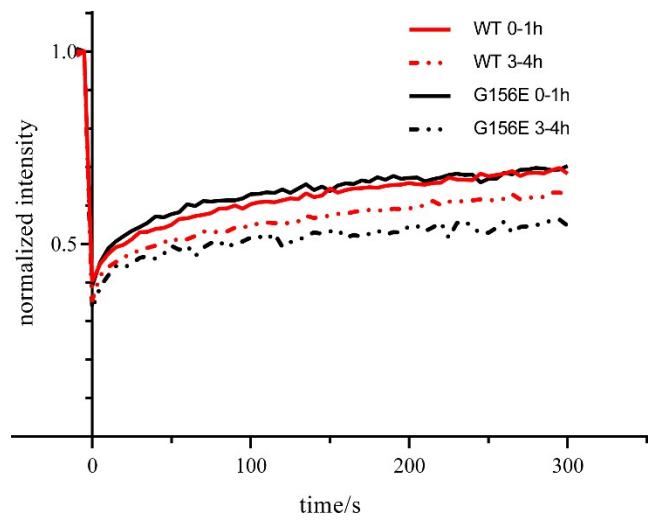


Figure S9. FRAP recovery curve of FUS-WT and its G156E mutant at different time.

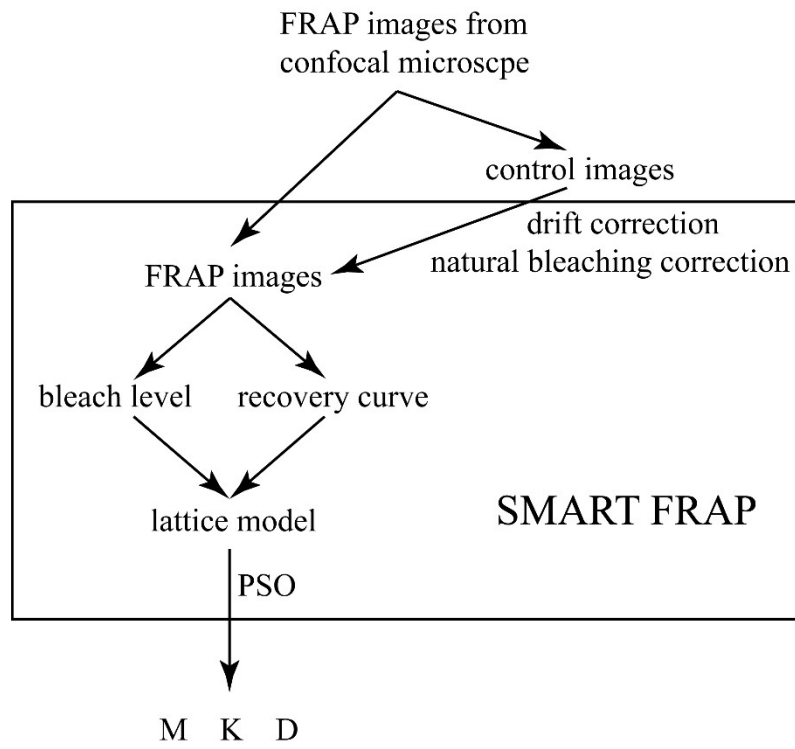


Figure S10. Flowchart of SMART FRAP.

1. H. C. Zhang, S. P. Shao, Y. Zeng, X. T. Wang, Y. Z. Qin, Q. N. Ren, S. Q. Xiang, Y. X. Wang, J. Y. Xiao and Y. J. Sun, *Nat Cell Biol*, 2022, **24**, 340-+.
2. J. Y. Tinevez, N. Perry, J. Schindelin, G. M. Hoopes, G. D. Reynolds, E. Laplantine, S. Y. Bednarek, S. L. Shorte and K. W. Eliceiri, *Methods*, 2017, **115**, 80-90.
3. N. O. Taylor, M. T. Wei, H. A. Stone and C. P. Brangwynne, *Biophysical Journal*, 2019, **117**, 1285-1300.
4. L. Hubatsch, L. M. Jawerth, C. Love, J. Bauermann, T. D. Tang, S. Bo, A. A. Hyman and C. A. Weber, *Elife*, 2021, **10**, e68620.
5. V. Wählstrand Skärström, A. Krona, N. Lorén and M. Röding, *J Microsc-Oxford*, 2021, **282**, 146-161.